JOURNAL OF Materials CHEMISTRY

Synthesis and characterisation of tin-doped iron oxides†

Frank J. Berry,*[a] Colin Greaves,[b] Örn Helgason[c] and Julia McManus[a]

[a] *Department of Chemistry, The Open University, Walton Hall, Milton Keynes, UK MK7 6AA*
[b] *School of Chemistry, The University of Birmingham, Edgbaston, Birmingham, UK B15 2TT*
[c] *Science Institute, University of Iceland, Dunhagi 3, 1S-107 Reykjavik, Iceland*

Received 6th April 1998, Accepted 22nd May 1998

Rietveld structure refinement of the X-ray powder diffraction data recorded from tin-doped Fe_3O_4 prepared by heating metallic iron, α-iron(III) oxide and tin(IV) oxide in sealed evacuated quartz ampoules shows the tin to substitute on the octahedral sites of the inverse spinel-related structure. Tin-doped γ-Fe_2O_3, prepared by boiling a precipitate derived from iron(III), iron(II) and tin(II) under reflux, also adopts an inverse spinel-related structure containing tin on the octahedral sites and, compared to pure γ-Fe_2O_3, is stabilised with respect to conversion to α-Fe_2O_3. ^{57}Fe Mössbauer spectroscopy shows the Neél temperature for γ-$Fe_{1.9}Sn_{0.1}O_3$ to be between 750 and 820 K. Tin-doped α-Fe_2O_3 prepared by hydrothermal methods is shown by Rietveld structure refinement of the X-ray powder diffraction data to contain tin in both the substitutional and interstitial octahedral sites of the corundum-related structure.

The doping of tetravalent titanium and tin into Fe_3O_4 and γ-Fe_2O_3[1–3] with the inverse spinel-related structure, and into α-Fe_2O_3 with the corundum-related structure[4–10] has been an area of activity for some time because of interest in the magnetic, electrical and other physical properties of the systems. The doping of Fe_3O_4 has attracted attention because of the possible use of the materials in transformer cores, magnetic memories and heterogeneous catalysts. The tin-doped α-Fe_2O_3 system is currently attracting interest because of its sensing properties for gases such as methane and carbon monoxide.[8,10–12] The preparation of the materials, their structural characterisation, and an understanding of the transformation of tin-doped variants of Fe_3O_4 to γ-Fe_2O_3 to α-Fe_2O_3 has been the subject of some uncertainty. We report here on the synthesis of tin-doped Fe_3O_4, γ-Fe_2O_3, and α-Fe_2O_3 by different methods, their structural characterisation and the influence of tin on some of their properties.

Experimental

Compounds of composition $Fe_{3-x}Sn_xO_4$ were prepared by heating stoichiometric quantities of powdered tin(IV) oxide, α-iron(III) oxide, and metallic iron in sealed evacuated quartz ampoules at 900 °C for 24 h and allowing the products to cool in the furnace. Compounds of the type γ-$Fe_{2-x}Sn_xO_3$ were prepared by adding aqueous ammonia to aqueous mixtures of iron(III) chloride hexahydrate, iron(II) chloride tetrahydrate, and tin(II) chloride until pH 7. The mixtures were boiled under reflux (3 h). The precipitates were removed by filtration, washed with 95% ethanol until no chloride ions could be detected in the washings by silver nitrate solution, and heated in air at 250 °C (12 h). Compounds of composition α-$Fe_{2-x}Sn_xO_3$ were prepared by precipitating aqueous mixtures of iron(III) chloride hexahydrate and tin(IV) chloride with aqueous ammonia and hydrothermally processing the precipitates in a Teflon-lined autoclave at 200 °C and 15 atm pressure for 5 h. The products were removed by filtration and washed with 95% ethanol until no chloride ions were detected by silver nitrate solution. The products were dried under an infrared lamp.

X-Ray powder diffraction (XRD) data were recorded with a Siemens D5000 diffractometer in reflection mode using Cu-Kα radiation. The program FULLPROF[13] was used for Rietveld refinement and simulation of patterns for specific structural models.

The tin K-edge extended X-ray absorption fine structure measurements were performed at the Synchrotron Radiation Source at Daresbury Laboratory UK with an average current of 200 mA at 2 GeV. The data were collected in transmission geometry on Station 9.2 at 298 K. The raw data were background-subtracted using the Daresbury programme EXBACK and fitted using the non-linear least squares minimisation programme EXCURV92 which calculates the theoretical EXAFS function using the fast curved wave theory.

The ^{57}Fe Mössbauer spectra were recorded from powdered samples with a constant acceleration spectrometer and a *ca.* 400 MBq ^{57}Co/Rh source. The furnace designed for the *in situ* study of phase transformations has been described in detail elsewhere.[14] The sample thickness was 50–80 mg cm^{-2}. The linewidth (FWHM) of the calibration spectrum was 0.24 mm s^{-1}. The chemical isomer shift data are quoted relative to the centroid of the metallic iron spectrum at room temperature.

Results and discussion

Tin-doped Fe_3O_4

X-Ray powder diffraction data were collected for a sample with nominal composition $Fe_{2.7}Sn_{0.3}O_4$. Given the large ionic size of Sn^{2+} ions, and their tendency to have irregular coordination owing to the influence of the lone-pair electrons, attention was focused on structural models involving the substitution of Sn^{4+} into the inverse spinel-related structure of Fe_3O_4. Of these, the strong preference of Sn^{4+} for octahedral stereochemistry suggested that models involving such substitution were most favoured. Charge compensation could be achieved by incorporating an equivalent concentration of either additional Fe^{2+} ions (0.3 per formula unit) or vacancies (0.1 per formula unit). X-Ray powder diffraction is suitable to differentiate between these, and other, models owing to the significant differences between the scattering factors of Fe and Sn ions. Since the sample had a minor contaminant (Fe_2SiO_4), a two-phase Rietveld structure refinement was performed. With respect to the primary magnetite phase, the results clearly supported a structure containing octahedral Sn^{4+} ions whose

†Basis of the presentation given at Materials Chemistry Discussion No. 1, 24–26 September 1998, ICMCB, University of Bordeaux, France.

Table 1 Refined structural parameters for $Fe_{2.7}Sn_{0.3}O_4$[a]

Atom	x/a	y/b	z/c	B/Å^2	Cell occupancy
Fe1	0.125	0.125	0.125	0.4(17)	8
Fe2	0.5	0.5	0.5	0.58(6)	13.44(15)
Sn	0.5	0.5	0.5	0.58(6)	2.56(15)
O	0.2569(5)	0.2569(5)	0.2569(5)	0.4(1)	32

[a]Space group *Fd3m*, $a=8.4936(3)$ Å; $R_{wp}=14.2\%$, $R_{exp}=11.8\%$, $R_1=3.9\%$.

charges are balanced by a corresponding excess of Fe^{2+} ions, and an excellent fit to the experimental data was obtained for this model. The refined structural parameters are given in Table 1, and the fitted XRD profile is shown in Fig. 1. The Fe1 sites are tetrahedrally coordinated and Fe2/Sn are octahedral. A single isotropic thermal parameter was assigned to the ions on the octahedral sublattice.

The unit cell is significantly larger than that of Fe_3O_4 ($a=8.396$)[15] which is consistent with the larger octahedral ionic radii of Fe^{2+} (0.78 Å) and Sn^{4+} (0.69 Å) compared with Fe^{3+} ions (0.65 Å).[16] The Sn:Fe ratio of 12(2)% is in good agreement with the nominal composition of the synthesised material (Sn/Fe = 11.1%).

We have reported previously[17] on how the ^{57}Fe Mössbauer spectra recorded from $Fe_{3-x}Sn_xO_4$ at temperatures between 300 and 790 K *in vacuo* enabled Curie temperatures, T_c, of 770 ± 5 K for $Fe_{2.9}Sn_{0.1}O_4$ and of 680 ± 10 K for $Fe_{2.8}Sn_{0.2}O_4$ to be calculated. Given that the Curie temperature[18] of Fe_3O_4 is 840 K, the results show that substitution by tin on the octahedral sites of Fe_3O_4 causes a progressive lowering of the Curie temperature. We have also described[19] how treatment of $Fe_{3-x}Sn_xO_4$ at moderate temperatures in air gives rise to γ-$Fe_{2-x}Sn_xO_3$.

Tin-doped γ-Fe_2O_3

The tin K-edge X-ray absorption fine structure (EXAFS) recorded from γ-$Fe_{1.9}Sn_{0.1}O_3$ and its Fourier transform are shown in Fig. 2. The results showed the tin to be coordinated by six oxygen atoms at 2.03 Å. The results demonstrate that the tin atoms in tin-doped γ-Fe_2O_3 adopt the octahedral, as opposed to tetrahedral, sites in the inverse spinel-related structure. The tin-oxygen distance compares well with that observed in tin dioxide of 2.041 Å (as also determined here by tin K-edge EXAFS and which is also consistent with data recorded by X-ray diffraction[20]).

In marked contrast to the refinement for tin-doped Fe_3O_4, X-ray powder diffraction was unable to yield definitive support for the substitution of tin into the structure of γ-Fe_2O_3. The small particle size due to the preparation method allowed refinement only of a simple structural model based on a cation deficient cubic spinel as opposed to the true tetragonally

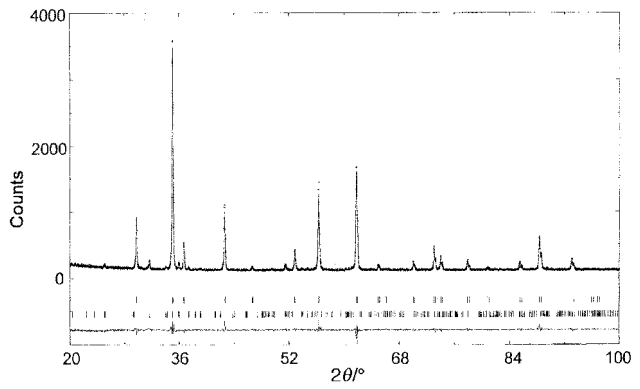

Fig. 1 Calculated and observed X-ray powder diffraction profiles for $Fe_{2.7}Sn_{0.3}O_4$.

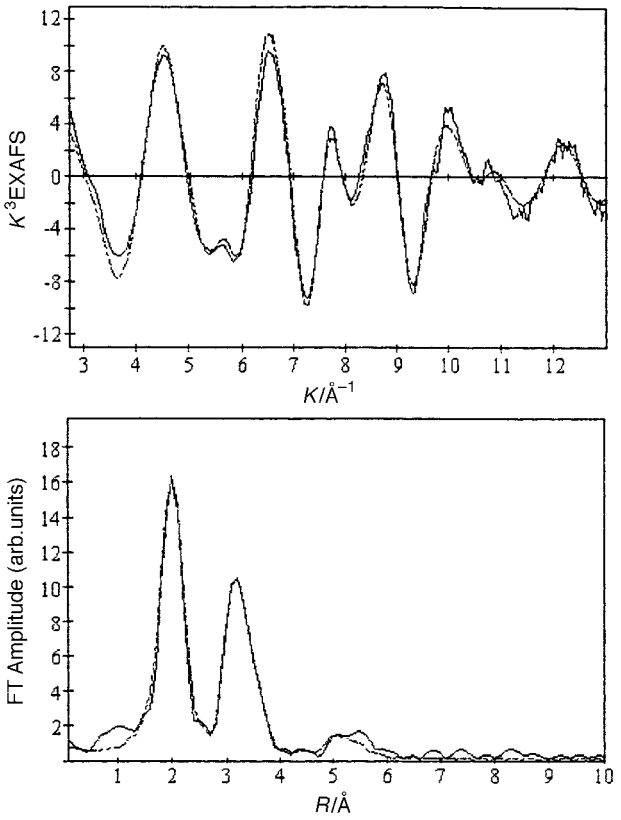

Fig. 2 Tin K-edge EXAFS and Fourier transform recorded from γ-$Fe_{1.9}Sn_{0.1}O_3$. The experimental data are indicated by the solid line.

distorted cell. Excellent fits to the XRD profiles were obtained using an unsubstituted γ-Fe_2O_3 model although the expansion of the unit cell [*e.g.* $a=8.356(1)$ Å for Sn/Fe = 0.05, compared to $a=8.334$ Å for γ-Fe_2O_3[21]] could relate to substitution of Sn^{4+} on the octahedral sites.

The X-ray powder diffraction patterns recorded from γ-Fe_2O_3 following heating at various temperatures to 477 °C are shown in Fig. 3. The results show the onset of conversion of γ-Fe_2O_3 to α-Fe_2O_3 at 377 °C and its virtual completion at 427 °C. In contrast, the X-ray powder diffraction patterns recorded from γ-$Fe_{1.9}Sn_{0.1}O_3$ (Fig. 4) demonstrate the stability of the tin-doped γ-Fe_2O_3 to conversion to tin-doped α-Fe_2O_3 up to 527 °C.

The ^{57}Fe Mössbauer spectra recorded from γ-$Fe_{1.9}Sn_{0.1}O_3$ between 25 and 557 °C (830 K) (Fig. 5) showed no evidence

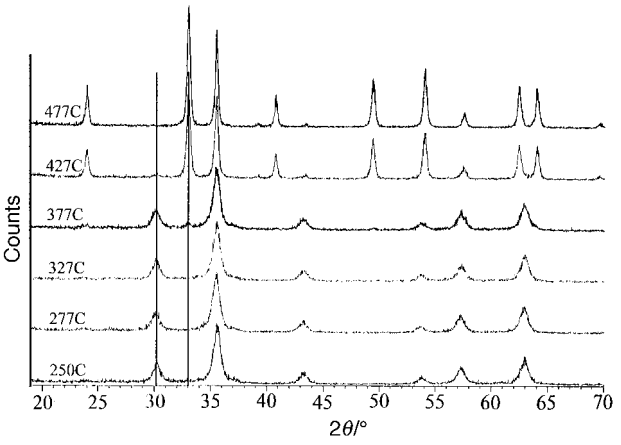

Fig. 3 X-Ray powder diffraction patterns recorded from γ-Fe_2O_3 heated at 250 °C (12 h) and between 277 and 477 °C for 20 h periods. The vertical lines indicate the demise of γ-Fe_2O_3 and the growth of α-Fe_2O_3 phases.

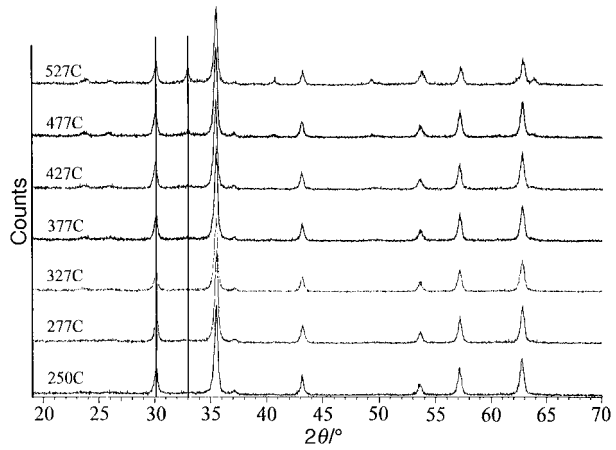

Fig. 4 X-Ray powder diffraction patterns recorded from γ-$Fe_{1.9}Sn_{0.1}O_3$ heated at 250 °C (12 h) and between 277 and 527 °C for 20 h periods. The vertical lines indicate the demise of γ-Fe_2O_3 and the growth of α-Fe_2O_3 phases.

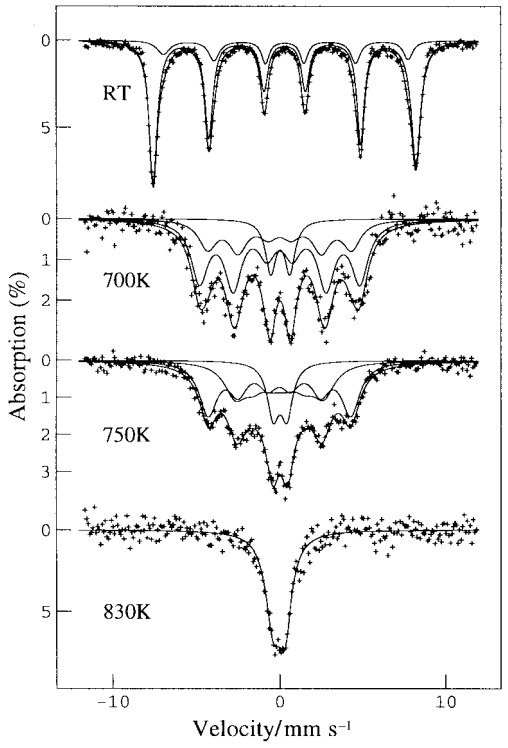

Fig. 5 ^{57}Fe Mössbauer spectra recorded *in situ* from γ-$Fe_{1.9}Sn_{0.1}O_3$ heated at 25 °C, 427 °C (6 h), 477 °C (21 h), and 557 °C (2 h).

for conversion of the γ-Fe_2O_3 to the α-Fe_2O_3 structure. The broad line spectrum recorded at 25 °C was fitted to a distribution of sextet patterns with 80% of the spectrum being related to magnetic hyperfine fields between 48.3 and 49.2 Tesla. This distribution reflects the influence of the Sn^{4+} ions on the magnetic interactions within γ-Fe_2O_3. The isomer shift (0.32–0.35 mm s^{-1}) confirms the presence of Fe^{3+} and the absence of quadrupole splitting is characteristic for γ-Fe_2O_3.

The spectrum recorded at 427 °C (700 K) remained dominated by a broad line sextet pattern with the magnetic field distributed between 26 and 30 T. The spectrum recorded at 477 °C (750 K) showed further reduction (and spreading) in the magnetic field (17 to 26 T) but also a doublet indicating that *ca.* 15% of the material had become paramagnetic. At 527 °C more than 90% of the spectrum corresponded to the paramagnetic species whilst the spectrum recorded at 557 °C (830 K) showed the material to be completely paramagnetic. The results show that γ-$Fe_{1.9}Sn_{0.1}O_3$ has a Neél temperature ranging between 477–547 °C (750–820 K) compared to 840–860 K for pure γ-Fe_2O_3 (an estimated value extrapolated from low temperature Mössbauer spectroscopy data due to the instability of γ-Fe_2O_3). Similar lowering was observed[17] in tin-doped Fe_3O_4. The wide temperature range of the Neél temperature in the present case may be associated with the distribution in particle size (44–66 nm as shown by scanning electron microscopy).

The material was subsequently heated to 587 °C (860 K) and the ^{57}Fe Mössbauer spectra recorded every 4 hours for a total heating period of 24 h. The first spectrum recorded between 4 and 8 h (Fig. 6) was fitted to a doublet characteristic of paramagnetic γ-Fe_2O_3. After further heating at 587 °C a magnetically split component began to emerge which was clearly observable in the spectrum recorded after 24 hours of heating. The hyperfine field of this sextet (23.5 T) and the quadrupole splitting (−0.1 mm s^{-1}) are characteristic of α-Fe_2O_3. The two spectra recorded on cooling to 427 °C (700 K) and 25 °C showed well defined patterns of two sextets. One of the sextet patterns can be related to the formation of tin-doped α-Fe_2O_3 with a magnetic field of 37.4 T at 427 °C (700 K) and 51.0 T at room temperature (in both cases the quadrupole splitting was −0.1 mm s^{-1}). The second sextet pattern corresponded to a residual amount (38% by area at room temperature) of tin-doped γ-Fe_2O_3 with a magnetic hyperfine field of 33 T at 427 °C (700 K) and 48.8 T at room temperature.

Tin-doped α-Fe_2O_3

The structural characteristics of tin-doped α-Fe_2O_3 prepared by hydrothermal methods have been investigated by Rietveld structure refinement of the X-ray powder diffraction data.[22] The analysis showed that the dopant ions occupy two distinct sites in the corundum-related structure of α-Fe_2O_3 in which the Fe^{3+} ions are distributed in an ordered fashion over 2/3 of the octahedral sites within a framework of hexagonally close-packed O^{2-} ions [Fig. 7(*a*)]. In this way chains of face-

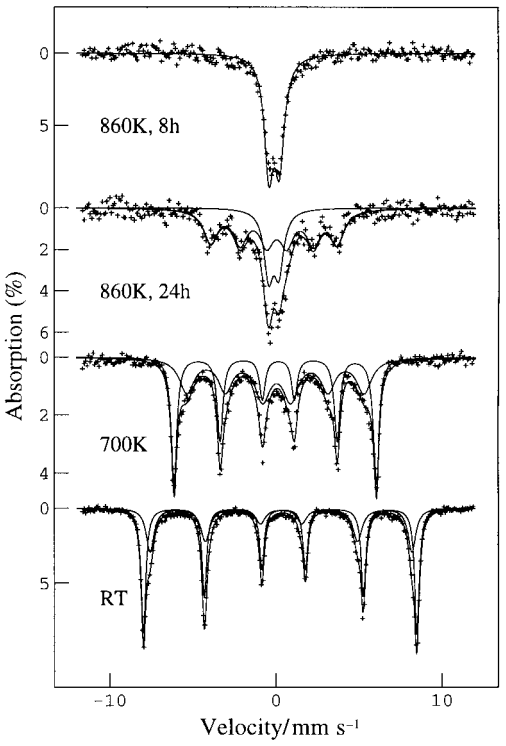

Fig. 6 ^{57}Fe Mössbauer spectra recorded *in situ* from γ-$Fe_{1.9}Sn_{0.1}O_3$ heated at 587 °C (4–8 h), 587 °C (20–24 h), and on cooling to 427 and 25 °C.

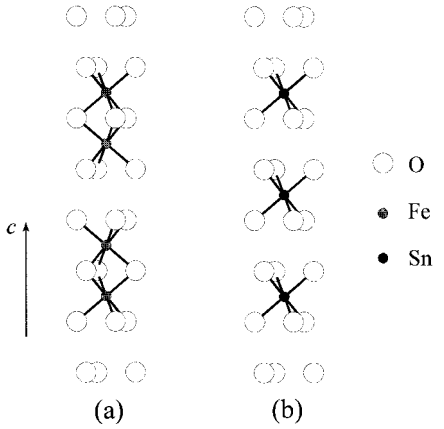

Fig. 7 (a) Linking of FeO_6 octahedra along *c* in α-Fe_2O_3. (b) Structural model involving the substitution of $4Fe^{3+}$ ions by $3Sn^{4+}$ ions.

sharing octahedra are directed along the *c*-axis and the Fe^{3+} ions within each chain form pairs. A simple model in which Sn^{4+} substituted for Fe^{3+} with charge balance being maintained by an appropriate number of cation vacancies would require the face-sharing of SnO_6 and FeO_6 octahedra which would be expected to be unstable due to high cation repulsion; in rutile-related SnO_2 only edge- and corner-shared octahedra occur. The best refinement to the X-ray powder diffraction data involved both interstitial *and* substitutional tin [Fig. 7(*b*)].[22] The presence of tin in the interstitial sites would produce strong cation–cation repulsions from the two adjacent face-shared FeO_6 octahedra. Elimination of the cations from these two sites results in two additional octahedral sites (respectively above and below the cations removed) which do not involve face-sharing and which are therefore attractive for occupation by additional tin ions. In this way the structural model shown in Fig. 7(*b*) was deduced: defect clusters are formed comprising a chain of three tin ions which all avoid face-sharing repulsions. In addition, the cluster is electrically neutral since $4Fe^{3+}$ ions are replaced by $3Sn^{4+}$ ions.

We thank the EPSRC for the award of a studentship (J.M.).

References

1 Ö. Helgason, H. P. Gunnlaugsson, S. Steinthorsson and S. Morup, *Hyperfine Interact.*, 1992, **70**, 981.
2 C. Djega-Mariadassou, F. Basile, P. Foix and A. Michel, *Ann. Chim.*, 1973, **8**, 15.
3 F. Basile, C. Djega-Mariadassou and P. Foix, *Mater. Res. Bull.*, 1973, **8**, 619.
4 F. J. Morin, *Phys. Rev.*, 1951, **83**, 1005.
5 N. Uekawa, M. Watanabe, K. Kaneko and F. Mizukami, *J. Chem. Soc., Faraday Trans.*, 1995, **91**, 2161.
6 P. B. Fabritchnyi, E. V. Lamykin, A. M. Babechkin and A. N. Nesmeianov, *Solid State Commun*., 1972, 11, 343.
7 F. Schneider, K. Melzer, H. Mehner and G. Deke, *Phys. Status Solidi A*, 1977, **39**, K115.
8 M. Takano, Y. Bando, N. Nakanishi, M. Sakai and H. Okinaka, *J. Solid State Chem.*, 1987, **68**, 153.
9 S. Music, S. Popovic, M. Metikos-Hukovic and G. Gvozdic. *J. Mater. Sci. Lett.*, 1991, **10**, 197.
10 H. Kanai, H. Mizutani, T. Tanaka, T. Funabiki, S. Yoshida and M. Takano, *J. Mater. Chem.*, 1992, **2**, 703.
11 P. Bonzi, L. E. Depero, F. Parmigiani, C. Perego, G. Sberveglieri and G. Quattroni, *J. Mater. Res.*, 1994, **9**, 1250.
12 Y. Liu, W. Zhu, M. S. Tse and S. Y. Shen, *J. Mater. Sci. Lett*., 1995, **14**, 1185.
13 J. Rodriguez-Carajal, 'FULLPROF' v.2.6.1' (ILL France), 1994; based on the original code by R. A. Young, *J. Appl. Crystallogr.*, 1981, **14**, 149.
14 Ö. Helgason, H. P. Gunnlaugsson, K. Jónsson and S. Steinthorsson, *Hyperfine Interact.*, 1994, **91**, 595.
15 B. A. Wechsler, D. H. Lindsley and C. T. Prewitt, *Am. Mineral.*, 1984, **69**, 754.
16 R. D. Shannon, *Acta Crystallogr., Sect. A*, 1976, **32**, 751.
17 F. J. Berry, Ö. Helgason, K. Jónsson and S. J. Skinner, *J. Solid State Chem.*, 1996, **122**, 353.
18 L. Häggstrom, H. Annersten, T. Ericson, R. Wäppling, W. Karner and S. Bjarman, *Hyperfine Interact.*, 1978, **5**, 201.
19 F. J. Berry, Ö. Helgason, K. Jónsson and S. J. Skinner, *Proceedings of the International Conference on the Applications of the Mossbauer Effect*, ed. I. Ortalli, SIF, Bologna, 1996, p. 59.
20 W. H. Bauer and A. A. Khan, *Acta Crystallogr., Sect. B*, 1971, **27**, 2133.
21 C. Greaves, *J. Solid State Chem.*, 1983, **49**, 325.
22 F. J. Berry, C. Greaves, J. G. McManus, M. Mortimer and G. Oates, *J. Solid State Chem.*, 1997, **130**, 272.

Paper 8/03861I